

Selected Papers from the 3rd Radiocarbon in the Environment Conference, Gliwice, Poland, 5–9 July 2021
© The Author(s), 2022. Published by Cambridge University Press for the Arizona Board of Regents on behalf of the University of Arizona. This is an Open Access article, distributed under the terms of the Creative Commons Attribution licence (<https://creativecommons.org/licenses/by/4.0/>), which permits unrestricted re-use, distribution, and reproduction in any medium, provided the original work is properly cited.

SCALING THE ^{14}C -EXCURSION SIGNAL IN MULTIPLE TREE-RING SERIES WITH DYNAMIC TIME WARPING

Irina Panyushkina^{1*}  • Valerie Livina² • Mihály Molnár³ • Tamas Varga³ • A J Timothy Jull^{3,4}

¹Laboratory of Tree-Ring Research, University of Arizona, Tucson, AZ 85721, USA

²Data Science Department, National Physical Laboratory, Teddington, TW11 0LW, UK

³Isotope Climatology and Environmental Research Centre (ICER), Institute for Nuclear Research, Debrecen 4026, Hungary

⁴Department of Geosciences and Department of Physics, University of Arizona, Tucson, AZ 85721, USA

ABSTRACT. A signal of rapid changes in ^{14}C production is logged in annual series of ^{14}C derived from tree rings, which can be associated with diverse effects of cosmic-ray fluxes, including solar burst and supernova events. These ^{14}C signatures may vary in time and space. The intensity and structure of the ^{14}C signal is multifaceted, which complicates understanding of the forcing and attribution of the underlying astrophysical events. It was suggested that $\Delta^{14}\text{C}$ in 1052/53 CE and 1054/55 CE signatures at a 4‰–6‰ range over two years could be caused by the Crab Nebula supernova (SN1054) or/and solar perturbation. The temporal incoherence of the signals in published ^{14}C series is investigated with dynamic time warping (DTW), novel approach for matching time-behavioral patterns in multiple ^{14}C datasets. DTW analysis of four ^{14}C signatures from tree rings of California, Finland and England suggests that ^{14}C spikes between 1052 CE and 1055 CE can be caused by a single event. The flickering fingerprint may result from cross-dating in conformity. Cross-checking of tree-ring records from distant locations is impossible sometimes due to large difference in environmental conditions limiting tree growth. The methodology helps to align the signals and can be applied to other ^{14}C datasets.

KEYWORDS: ^{14}C excursions, DTW method, SEP, supernova, tree rings.

INTRODUCTION

The annual rate of ^{14}C production in the lower stratosphere-upper troposphere reflects the changes in cosmic-ray flux over time due to changes in the intensity of galactic cosmic rays and solar energetic particles, and solar-geomagnetic shielding (Burr 2007). Variations of the ^{14}C production rate are present in time series that can be derived from various terrestrial archives. Yet, annual series of ^{14}C from tree rings are considered superior tracers of the ^{14}C signal in time and space, since trees continuously use carbon dioxide gas from the air and ground water during photosynthesis, and distribution of the carbon isotopes has been almost completely mixed and homogenized over the globe (Poluianov et al. 2016; Wu et al. 2018).

So far, three confirmed solar energetic particle events (SEP 774 CE, 993 CE, 660 BCE, and 7176 BCE), one supernova (SN1056) and proposed solar-proton event (5259 BCE) have been confirmed with annual ^{14}C series from numerous geographical locations and different AMS radiocarbon laboratories (Jull et al. 2014; Fogtmann-Schulz et al. 2017; Büntgen et al. 2018; Terrasi et al. 2020; Sakurai et al. 2020; Brehm et al. 2021a; Paleari et al. 2022). Four other proposed ^{14}C excursions (1279 CE, 813 BCE, 5480 BCE, and 5410 BCE) need to be corroborated with data from multiple locations or need to be confirmed (Miyake et al. 2017, 2021; Jull et al. 2018; Brehm et al. 2021b).

*Corresponding author: Email: ipanyush@arizona.edu

It is known that manifestations of the same astrophysical event in carbon-14 may occur with delays in timing and variation in intensity across different parts of the globe. Büntgen et al. (2018) clearly demonstrated the meridional decline of 11-year mean atmospheric ^{14}C concentrations across the northern and southern hemispheres in a case study of SEP 774 CE and 993 CE. Studies of possible supernova events have been hampered by inconclusive patterns in the ^{14}C signal response due to smaller effects than in the SEP cases and temporal discord in the variation of $\Delta^{14}\text{C}$ (Dee et al. 2016; Eastoe et al. 2019; Brehm et al. 2021b). Yet, the increase of production rate in the ^{14}C signatures around supernova appearances cannot be explained by the Schwabe cycle alone (Terrasi et al. 2020; Brehm et al. 2021b). It seems that the SN-signal in the rapid change in ^{14}C production is less comprehensible and different from highly coherent SEP-signal in $\Delta^{14}\text{C}$ series forced by solar proton radiation.

The γ -ray burst produced by a supernova explosion arrives to the Earth at the same time as the visible light, which is documented by historical archives describing the appearance of a guest or new star (Pavlov et al. 2013). The mean interval between supernova events in the Milky Way galaxy is not that long and is estimated at 40 years \pm 10 yr (Tammann et al. 1994). Cosmic rays accelerated at supernova remnant shocks change the chemistry of the atmosphere through ionization and dissociation of O_3 and N_2 which lead to the formation of nitrogen oxide compounds (Thomas and Melott 2006). Damon et al. (1995) searched for the effects of γ -ray bursts produced by supernovae in ^{14}C records and determined an upper limit of 6‰ in $\Delta^{14}\text{C}$ for a large SN event within our Galaxy (Damon et al. 1995). Back then the error of ^{14}C measurements produced by beta-counting systems used to be high around 4‰ (Cook and van der Plicht 2013). The precision of modern AMS ^{14}C measurements has significantly improved the errors and reduced the estimate for the background concentration to 1.3–2‰ (Wacker et al. 2010). The AMS records and the finer temporally resolved series of ^{14}C from tree rings may assist in improving the attribution of SN signal in ^{14}C series.

A recent investigation of the effect of the Crab Nebula supernova (SN1054) in the annual rate of ^{14}C production found a $\Delta^{14}\text{C}$ excursion at 1054/55 CE of 4‰ at tree-ring archives from Sierra Nevada Mountains and Finnish Lapland (Terrasi et al. 2020). However, other studies of tree rings from Central England and another location in the Sierra Nevada Mountains (California) report much higher ^{14}C ranges for this time interval (up to 6‰) but in 1053 CE, one year prior to the SN1054 visible light arrival to the Earth atmosphere, and attribute it to a possible SEP event (Eastoe et al. 2019; Brehm et al. 2021b). Brehm et al. (2021b) suggested this designation for a 6‰ change from 1052 CE to 1053 CE (1 yr) or a ca. 8‰ variation from 1052 CE to 1055 CE (3 yr). This research points to the interval 1052–1055 CE that may have two separate ^{14}C spikes causes by two different cosmic events. Interestingly, some tree-ring series did not show any significant rise in $\Delta^{14}\text{C}$ at that time (see Gütthler et al. 2013) and others record a slight intensification of ^{14}C production (Menjo et al. 2005). Dee et al. (2016) examined the $\Delta^{14}\text{C}$ response in tree-ring series covering the timing of four historical supernovae and found no significant increase in $\Delta^{14}\text{C}$ tree-ring series around 1054 CE. It appears that the SN signature in annual ^{14}C series is more difficult to identify than SEP signatures.

In this paper, we employ a novel technique of dynamic time warping (DTW) to ^{14}C annual series in order to investigate the temporal coherence of the published ^{14}C series for 1053(52)–55CE signature from four tree-ring archives at three locations (Finland,

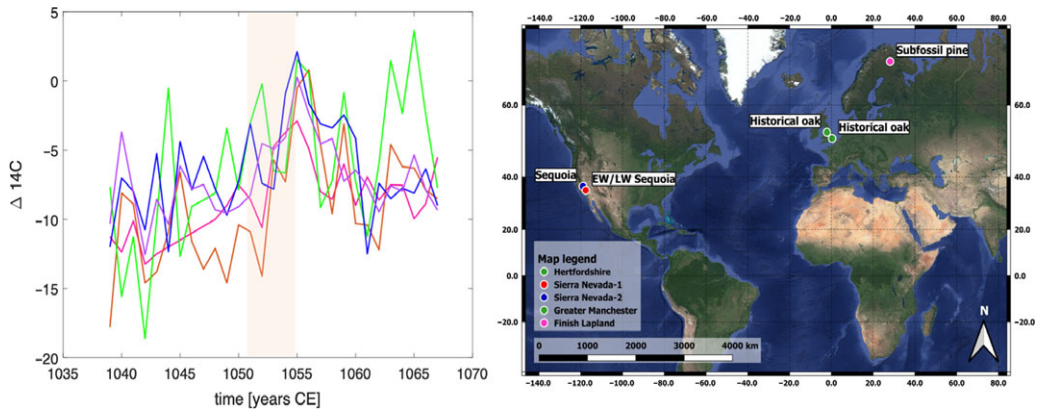


Figure 1 ^{14}C dataset used in the study. Left: annual series of $\Delta^{14}\text{C}$ attributed to possible SN1054 or SEP events. Color code of the curves: red—Full Ring Sequoia (Seq) from Eastoe et al. (2019); blue—EW Seq, brown—LW Seq and magenta—Finnish Pine from Terrasi et al. (2020); green—English oak from Brehm et al. (2021b). Shaded area is the signature interval 1052–1055 CE. Right: map of the tree-ring data locations. (See online version for color figures.)

California, and England) from published literature (Brehm et al. 2021b; Eastoe et al. 2019; Terrasi et al. 2020). The DTW algorithm performs matching of similar patterns in datasets that may not be coeval. The method allows stretching or compressing sub-sections of the time axis at different scales to minimize and quantify the dissimilarity between the compared time series, as discussed by Izakian et al. (2015).

METHODS

We evaluate the temporal coherence of five ^{14}C series with 1052 CE/1054 CE signatures developed independently and published by Eastoe et al. (2019), Terrasi et al. (2020), and Brehm et al. (2021b) (Figure 1a). The tree rings are originated from four locations (Figure 1b). At one location we measured ^{14}C in earlywood (EW) and latewood (LW) of the rings separately. Supplementary material includes the original ^{14}C datasets used in this study. All details concerning the tree-ring sampling, ^{14}C measurements and $\Delta^{14}\text{C}$ calculation can be found in the relevant publications. The records of three tree species are positioned in the coordinate box 36°N , 68°N and 118°W , 28°E , with an elevational gradient between 191 m asl and 1890 m asl (Figure 1b). The wood is sourced from living trees (sequoia), buried subfossils (pine) and historical timber (oak). The tree-ring records of *Sequoiadendron giganteum* come from two nearby sites in the Sierra Nevada Mountains, California (36.56°N , 118.75°W , 1890 m asl and 36.75°N , 118.97°W , 1850 m asl), *Pinus sylvestris* from Finnish Lapland (68.31°N , 28.09°E , 191 m asl) and English oak from the UK historical buildings near Hertfordshire and Greater Manchester with unknown harvesting locations in the area (51.75°N , 0.34°W for STA-C34 specimen and 53.41°N , 2.15°W for STK-C10 specimen). Annually resolved ^{14}C data in addition to one location with sub-annually earlywood and latewood series of sequoia were examined for the period 1037–1067 CE (30 yr) with DTW.

DTW is an approach of machine learning (ML) and artificial intelligence (AI) for data analysis that is gaining popularity with increasing computational power, although many of the ML and AI techniques were developed in the 1960s–1980s. DTW was introduced by Sakoe and Chiba (1978) for spoken-word recognition, where a warping time function is used for optimal

dynamic programming. Paliwal et al. (1982) proposed an improvement of the method with removal of the warping function slope constraints. Recent improvements introduced weights for uncertainty accounting (see Zuo and Yan 2018). DTW is a generalization of a point-wise comparison of records based on Euclidean distance. Instead of “rigid” comparison of correlation, DTW allows “elastic” matching of patterns by means of minimizing the differences between time series with added time intervals, thus allowing variability in time by means of DTW alignment.

We use the Matlab built-in function for implementation of DTW (<https://uk.mathworks.com/help/signal/ref/dtw.html>) that performs the pairwise transformation and synchronization of time series as described in Aribas-Gil and Muller (2014). In our context, the pairs of time series are the tree-ring ^{14}C series to be compared. Our goal is to achieve the *alignment* of the time series with optimized matching of the entire sequence (Aribas-Gil and Muller 2014). Given two time series $A = (a_1, \dots, a_n)$ and $B = (b_1, \dots, b_m)$, we construct an $n \times m$ matrix of Euclidean distances of all pairs of (i, j) between the elements of A and B . The warping path W is a set the matrix elements $W = (w_1, \dots, w_k)$, $\max(m, n) \leq K \leq m + n - 1$, satisfying the boundary condition and conditions of continuity and monotonicity required of a path (and there are multiple paths of this kind). The optimal path is obtained as

$$DTW(A, B) = \operatorname{argmin}_{W=w_1, \dots, w_k} \sqrt{\sum_{k=1}^K (a_i - b_j)^2}$$

where A and B are two ^{14}C series, a and b refer to the ^{14}C values, w represents time weights that account for the optimized alignment, k is the index of the alignment pairs. The DTW algorithm measures similarity between time series where oscillations vary in speed and power. In principle, this method can evaluate time-series variance over a period of several decades to several thousand years. We hypothesize that the cosmic excursion effect could be detected in $\Delta^{14}\text{C}$ series from years with extreme variance such as year-to-year spikes. The DTW approach aligns the selected ^{14}C series that register similar signal within different time-response window. Analyzing the dynamics of time series of interest with shape-based DTW distance determines a close relationship between the time series exhibiting a similar patterns in ^{14}C production rate presented in tree rings at different years.

RESULTS

The studied signature in the annual ^{14}C series appears as a rapid increase of $\Delta^{14}\text{C}$, the peak is sustained for the next one to two years and is followed by a 2-yr decay (Figure 1a). The range of $\Delta^{14}\text{C}$ in the signature varies from -10.59‰ and -7.83‰ (1052–53 CE) and -2.9‰ and -0.91‰ (1054–55 CE). The standard deviation (1σ) for the sequoias and Finnish pine series is typical between 2‰ and 2.09‰ . The English oak series has a much smaller measurement error of 1.13‰ – 1.6‰ . The increment of $\Delta^{14}\text{C}$ at the first-year increase is between 7.5‰ and 3.8‰ , which is a significant change. However, the peak signature occurs at different year: 1054 CE or 1055 CE. Brehm et al. (2021b) named the signature “1052 CE event” observed in the English oak and Full-Ring Sequoia (Eastoe et al. 2019). Its attribution to a possible SEP occurred during the Oort solar minimum (1021–1060 CE) has yet not been confirmed, while Terrasi et al. (2020) attributed a similar-structured signature with 1-yr shift from three ^{14}C series possibly to γ -rays from the Crab Nebula supernova (SN1054), an unusually weak solar minimum or a SEP.

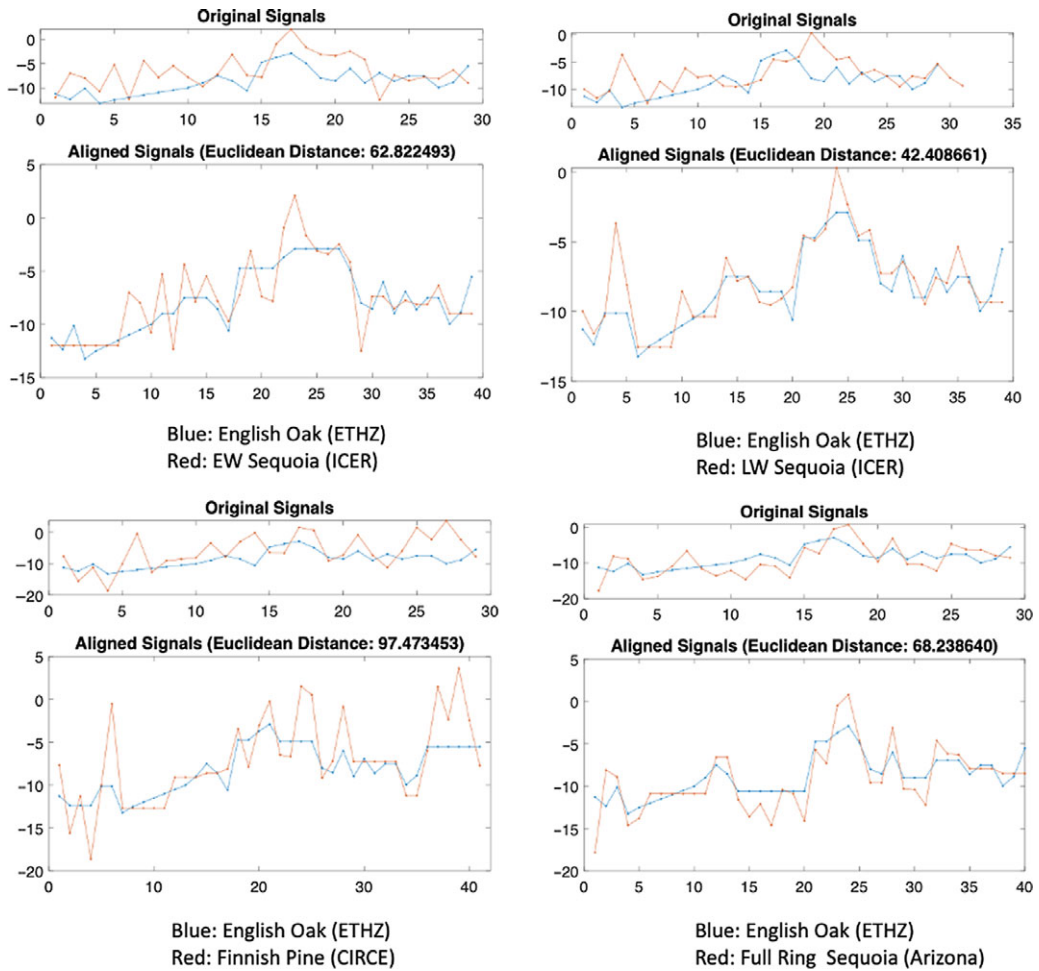


Figure 2 DTW-matching of 1054 CE event/1052 CE-event signal between the English oak (blue line) and other (red line) studied locations and AMS facilities: Isotope Climatology and Environmental Research Centre, Debrecen, Hungary (ICER), Center for Isotopic Research on the Cultural and Environmental heritage University of Naples, Italy (CIRCE), NSF-Arizona AMS facility, University of Arizona, USA (Arizona), Laboratory of Ion Beam Physics, Swiss Federal Institute of Technology in Zürich, Switzerland (ETHZ). In each of four blocks of the figure, the top panels display the original series to be compared for the interval 1038–1068 CE. The low panels show the best global alignment of the signal between ^{14}C annual series with added time points. (See online version for color figures.)

We applied DTW to compare the 1054 CE event versus the 1052 CE event in pairing ^{14}C tree-ring time series over the 30-yr interval: 1037–1067 CE. Firstly, the English oak ^{14}C series was paired with four other ^{14}C sets. Figure 2 shows the original series and globally aligned-signal series with the calculated Euclidean distance. Second, we aligned the ^{14}C series of sequoia from California (EW, LW, and Full Ring). Figure 3 shows the best aligned series from this test. Finally, the sequoia and Finnish pine ^{14}C series were processed in the same way (not shown). DTW is often used as a distance measure (not a norm, as the triangular inequality is not fulfilled) in cauterization of time series sets (Kate 2016). The DTW analysis suggests that the signatures of 1054 CE event and 1052 CE event are matching and manifest the same pattern in the studied time series, but they do not coincide

Table 1 Euclidean distance between DTW paired ^{14}C series. Seq refers to Sequoia.

^{14}C series	Finnish Pine	English Oak	EW Seq	LW Seq
English Oak	97.43			
EW Seq	84.87	62.82		
LW Seq	90.25	42.41	42.32	
Full Ring Seq	95.51	68.24	63.2	70.39

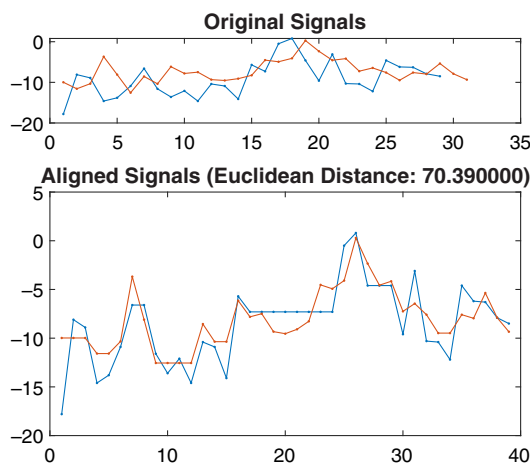


Figure 3 DTW-matching of 1054CE event/1052 CE event signal between Sequoia series from two locations in California and two AMS labs. The top panel displays the original series, and the bottom plot denotes the best global alignment of the signal in the paired ^{14}C annual series with added time points. (See online version for color figures.)

in time. Moreover, the ^{14}C time series from Finnish pine has the closest relation to all series, while the English oak and LW Sequoia are most remote time series (Table 1). Instead of a “rigid” comparison, DTW allows “elastic” matching of signals with minimization of the differences between time series via added time intervals, thus allowing the alignment of variance. Sequoia ^{14}C series of EW and LW from the same ring demarcate two different $\Delta^{14}\text{C}$ patterns that can be aligned by DTW (Figure 3). The difference in the ^{14}C variance of these series possibly results from the different time scales. Early wood is mostly responsive to May–June moisture driving by the snowmelt, while the late wood formation occurs in July–August extremely dry season (Hughes and Brown 1992).

Analysis of the lagged cross-correlation for the ^{14}C series suggests that there is a two-year lag between the English oak and California EW–LW sequoia series (Figure 4, right plot). Perhaps, this two-year offset is caused by cross-dating nonconformity between these two tree-ring chronologies. It is surprising that the 1052 CE event signal showed up in other California sequoia record since its chronology matched well with the EW and LW sequoia records with the 1054 CE signal. DTW analysis demonstrates that ^{14}C variance amplification at both 1052 CE and 1054 CE is caused by the impact of a single event. The inconsistent

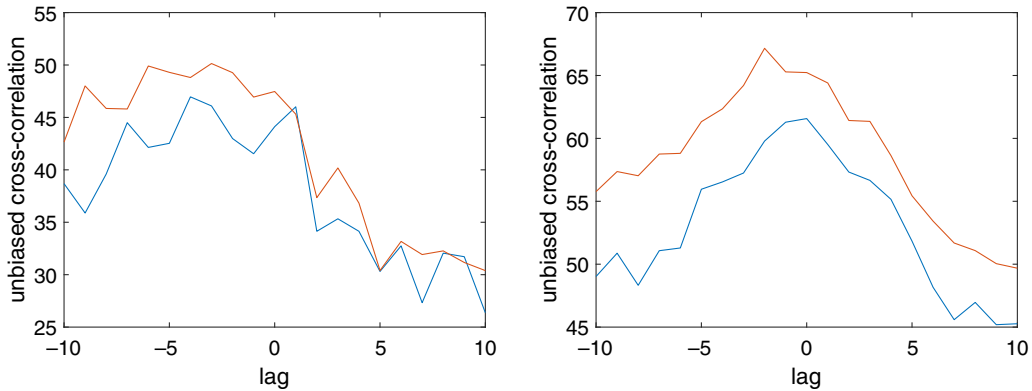


Figure 4 Cross-correlation of considered time series at different lags. Left panel: cross-correlation between Finnish pine and EW Sequoia (blue line) and between Finnish pine and LW Sequoia (red line). Right panel: cross-correlation between English oak and EW Sequoia (blue line) and between English oak and LW Sequoia (red line). The sharp peaks denote the lags at which the time series have the highest cross-correlations confirming the DTW analysis and the shift in the timing of the ^{14}C events. (See online version for color figures.)

fingerprint of the 1054 CE event in time across the space may result from cross-dating nonconformity, regional (local) flux of old carbon at the northern site (Finland) due to intensified permafrost melt and ancient CO_2 release when the tree grew during the Medieval Warm Epoch (Feng et al. 2013; Wild et al. 2019; Zhang et al. 2021) and/or large latitude gradient (e.g., Burr 2007; Büntgen et al. 2018; Uusitalo et al. 2018). Clearly, the 1052–1054 CE signature is a unique increase in ^{14}C production rate and warrants further investigation.

CONCLUSIONS

Our first-time application of a DTW approach to ^{14}C annual datasets has shown that it is possible to scale and match similar patterns in the $\Delta^{14}\text{C}$ variance with the signal placed chronologically apart and originated by an astrophysical impact (γ -ray or solar protons). DTW analysis effectively measures the distance with respect of signal separated in time. Temporal separation of the signal can be attributed to complex cross-dating of various wood sources and continues progress in the development of multimillennial tree-ring chronologies. Another source of transient errors can arise from instrumental bias and occur during ring sampling, cellulose processing, and digitization of datasets.

Whatever the reason for the chronological divergence of signals, DTW can identify divergencies of the discording signals. Our DTW analyses demonstrates an effective way of determining the distance between individual ^{14}C series (points in space) with focusing on the similarity of their temporal (not chronological) behavior. In this case study, we cannot attribute the observed ^{14}C signature between 1052/53–1056 CE to either SN1054 or a possible SEP event. Moreover, this signature and the offset in the ^{14}C production rate should be revisited and investigated with larger spatial datasets.

ACKNOWLEDGMENTS

This research was supported in part by U.S. NASA Grant # 80NSSC21K1426 and the European Union and the State of Hungary co-financed by the European Regional

Development Fund in the project of GINOP-2.3.4-15-2020-00007 “INTERACT”. The ICER lab was co-financed by the European Regional Development Fund project # GINOP-2.3.2-15-2016-00009 ICER.

CONFLICT OF INTEREST

Dr. Jull has disclosed an outside interest in Hungarian and Czech Academies of Sciences to the University of Arizona. Conflicts of interest resulting from this interest are being managed by the University of Arizona in accordance with its policies.

SUPPLEMENTARY MATERIAL

To view supplementary material for this article, please visit <https://doi.org/10.1017/RDC.2022.25>

REFERENCES

- Arribas-Gil A, Mueller H. 2014. Pairwise dynamic time warping for event data. *Computational Statistics and Data Analysis* 69:255–268.
- Brehm N, Christl M, Adolphi F et al. 2021a. Tree rings reveal two strong solar proton events in 7176 and 5259 BCE. Preprint doi: [10.21203/rs.3.rs-753272/v1](https://doi.org/10.21203/rs.3.rs-753272/v1).
- Brehm N, Bayliss A, Christl M, Synal H-A, Adolphi F, Beer J, Kromer B, Muscheler R, Solanki SK, Usoskin I, Bleicher N, Bollhalder S, Tyers C, Wacker L. 2021b. Eleven-year solar cycles over the last millennium revealed by radiocarbon in tree rings. *Nature Geoscience* 14:10–15. doi: [10.1038/s41561-020-00674-0](https://doi.org/10.1038/s41561-020-00674-0).
- Büntgen U and others. 2018. Tree rings reveal globally coherent signature of cosmogenic radiocarbon events in 774 and 993 CE. *Nature Communication* 9:3605. doi: [10.1038/s41467-018-06036-0](https://doi.org/10.1038/s41467-018-06036-0).
- Burr GS. 2007. Radiocarbon dating: causes of temporal variations. In: Elias SA, Mock CJ editors. *Encyclopedia of Quaternary science*. Oxford: Elsevier. p. 2931–2941. doi: [10.1016/B0-44-452747-8/00044-2](https://doi.org/10.1016/B0-44-452747-8/00044-2).
- Cook GT, van der Plicht J. 2013. Radiocarbon dating—conventional method. In: Elias SA, Mock CJ, editors. *Encyclopedia of Quaternary science*. 2nd edition. 305–315. Amsterdam: Elsevier. doi: [10.1016/B978-0-444-53643-3.00048-0](https://doi.org/10.1016/B978-0-444-53643-3.00048-0).
- Damon PE, Kaimei D, Kocharov GE, Mikheeva IB, Peristykh AN. 1995. Radiocarbon production by the gamma-ray component of supernova explosions. *Radiocarbon* 37(2):599–604.
- Dee MW, Pope B, Miles D, Manning S, Miyake F. 2016. Supernovae and single-year anomalies in the atmospheric radiocarbon record. *Radiocarbon* 59(2):293–302.
- Eastoe CJ, Tucek CS, Touchan R. 2019. $\Delta^{14}\text{C}$ and $\delta^{13}\text{C}$ in annual tree-ring samples from *Sequoiadendron Giganteum*, AD 998–1510: solar cycles and climate. *Radiocarbon* 61(3):661–680. doi: [10.1017/RDC.2019.27](https://doi.org/10.1017/RDC.2019.27).
- Feng X, Vonk JA, van Dongen BE, Gustafsson O, Semiletov IP, Dudarev OV, Wang Z, Montluçon DB, Wacker L, Eglinton TI. 2013. Differential mobilization of terrestrial carbon pools in Eurasian Arctic river basins. *PNAS* 110(35):14168–14173. doi: [10.1073/pnas.1307031110](https://doi.org/10.1073/pnas.1307031110).
- Fogtmann-Schulz A, Østbø SM, Nielsen SGB, Olsen J, Karoff C, Knudsen MF. 2017. Cosmic-ray event in 994 CE recorded in radiocarbon from Danish Oak. *Geophysical Research Letters* 44(16):8621–8628. doi: [10.1002/2017GL074208](https://doi.org/10.1002/2017GL074208).
- Güttler D, Wacker L, Kromer B, Friedrich M, Synal H-A. 2013. Evidence of 11-year solar cycles in tree rings from 1010 to 1110 AD—progress on high precision AMS measurements. *Nuclear Instruments and Methods in Physics Research B* 294:459–463.
- Hughes MK, Brown PM. 1992. Drought frequency in central California since 101 B.C. recorded in giant sequoia tree rings. *Climate Dynamics* 6(3–4): 161–167.
- Izakian H, Pedrycz W, Jamal I. 2015. Fuzzy clustering of time series data using dynamic time warping distance. *Engineering Appl. Artificial Intelligence* 39:235–244.
- Jull AJT, Panyushkina IP, Lange TE, Kukarskih VV, Clark KJ, Myglan VS, Salzer M, Burr GS, Leavitt SL. 2014. Excursions in the ^{14}C record at AD 774–775 from tree rings from Russia and America. *Geophysical Research Letters* 41(8):3004–3010. doi: [10.1002/2014GL059874](https://doi.org/10.1002/2014GL059874).
- Jull AJT, Panyushkina IP, Miyake F, Masuda K, Nakamura T, Lange TE, Cruz RJ, Baisan C, Janovics R, Varga T, Molnár M. 2018. More rapid carbon-14 excursions in the tree-ring

- record: A record of different kind of solar activity at about 800 BC? *Radiocarbon* 60(4): 1237–1248. doi: [10.1017/RDC.2018.53](https://doi.org/10.1017/RDC.2018.53).
- Kate R. 2016. Using dynamic time warping distances as features for improved time series classification. *Data Mining and Knowledge Discovery* 30(2): 283–312.
- Miyake F, Jull AJT, Panyushkina IP, Wacker L, Salzer M, Baisan C, Lange T, Cruz R, Masuda K, Nakamura T. 2017. Large ^{14}C excursion in 5480 BC indicates an abnormal sun in the mid-Holocene. *PNAS Physical Sciences—Earth, Atmospheric, and Planetary Sciences* 114 (5): 881–884. doi: [10.1073/pnas.1613144114](https://doi.org/10.1073/pnas.1613144114).
- Miyake F, Panyushkina IP, Jull AJT, Helama S, Kanzawa K, Moriya T, Nicolussi K, Oinonen M, Salzer M, Tokanai F, Takeyama M, Wacker L. 2021. A single-year cosmic ray event of 5410 BCE registered in ^{14}C of tree rings. *Geophysical Research Letters* 48 (11):e2021GL093419. doi: [10.1029/2021GL093419](https://doi.org/10.1029/2021GL093419).
- Menjo H, Miyahara H, Kuwana K, Masuda K, Muraki Y, Nakamura T. 2005. Possibility of the detection of past supernova explosion by radiocarbon measurement. *International Cosmic Ray Conference* 2:357.
- Paleari CI, Mekhaldi F, Adolphi F et al. 2022. Cosmogenic radionuclides reveal an extreme solar particle storm near a solar minimum 9125 years BP. *Nature Communication* 13(214). doi: [10.1038/s41467-021-27891-4](https://doi.org/10.1038/s41467-021-27891-4).
- Paliwal K, Agarwal A, Sinha S. 1982. A modification over Sakoe and Chibas dynamic time warping algorithm for isolated word recognition. *Signal Processing* 4(4):329–333.
- Pavlov AK, Blinov AV, Vasilyev GI, Vdovina MA, Volkov PA, Konstantinov AN, Ostryakov VM. 2013. Gamma-ray bursts and the production of cosmogenic radionuclides in the Earth's Atmosphere. *Astronomy Letters* 39(9):571–577.
- Poluianov SV, Kovaltsov GA, Mishev AL, Usoskin IG. 2016. Production of cosmogenic isotopes ^7Be , ^{10}Be , ^{14}C , ^{22}Na , and ^{36}Cl in the atmosphere: altitudinal profiles of yield functions. *J. Geophys Res Atmos* 121:8125–8136. doi: [10.1002/2016JD025034](https://doi.org/10.1002/2016JD025034).
- Sakoe H, Chiba S. 1978. Dynamic programming algorithm optimization for spoken word recognition. *IEEE Transactions on Acoustics, Speech and Signal Processing ASSP*-26:1.
- Sakurai H, Tokanai F, Miyake F et al. 2020. Prolonged production of ^{14}C during the ~660 BCE solar proton event from Japanese tree rings. *Scientific Reports* 10:660. doi: [10.1038/s41598-019-57273-2](https://doi.org/10.1038/s41598-019-57273-2).
- Tammann GA, Löffler W, Schröder A. 1994. The galactic supernova rate. *Astrophysical Journal Supplement Series* 92:487–493.
- Terrasi F, Marzaioli F, Passariello I, Porzio G, Capano M, Helama S, Oinonen M, Nöjd P, Uusitalo J, Jull AJT, Panyushkina IP, Baisan C, Molnar M, Kovaltsov G, Poluianov S, Usoskin I. 2020. Can the ^{14}C anomaly in 1054 CE be due to SN1054? *Radiocarbon*. doi: [10.1017/RDC.2020.58](https://doi.org/10.1017/RDC.2020.58).
- Thomas BC, Melott AL. 2006. Gamma-ray bursts and terrestrial planetary atmospheres. *New Journal of Physics* 8(7):120. doi: [10.1088/1367-2630/8/7/120](https://doi.org/10.1088/1367-2630/8/7/120).
- Uusitalo J, Arppe L, Hackman T et al. 2018. Solar superstorm of AD 774 recorded subannually by Arctic tree rings. *Nature Communication* 9:3495. doi: [10.1038/s41467-018-05883-1](https://doi.org/10.1038/s41467-018-05883-1).
- Wacker L, Bonani G, Friedrich M, Hajdas I, Kromer B, Nemeč M, Ruff M, Suter M, Synal H-A, Vockenhuber. 2010. MICADAS: routine and high-precision radiocarbon dating. *Radiocarbon* 52(2–3):252–262. doi: [10.1017/S0033822200045288](https://doi.org/10.1017/S0033822200045288).
- Wild B, Andersson A, Bröder L, Vonk J, Hugelius G, McClelland JW, et al. 2019. Rivers across the Siberian Arctic unearth the patterns of carbon release from thawing permafrost. *PNAS* 116(21):10280–10285. doi: [10.1073/pnas.1811797116](https://doi.org/10.1073/pnas.1811797116).
- Wu C-J, Usoskin I, Krivova N, Kovaltsov G, Baroni M, Bard E, Solanki S. 2018. Solar activity over nine millennia: A consistent multi-proxy reconstruction. *Physics, Astronomy & Astrophysics: A&A* 615, A93. doi: [10.1051/0004-6361/201731892](https://doi.org/10.1051/0004-6361/201731892).
- Zhang X, Bianchi TS, Hanna AJM, Shields MR, Izon G, Hutchings JA, Ping C-L, Kanevskiy M, Haghypour N, Eglinton TI. 2021. Recent warming fuels Increased organic carbon export from Arctic permafrost. *AGU Advances* 2(2):e2021AV000396. doi: [10.1029/2021AV000396](https://doi.org/10.1029/2021AV000396).
- Zuo L, Yan L. 2018. A weighted DTW approach for similarity matching over uncertain time series. *Journal of Computing and Information Technology* 26(3):179–190.